ANALYSIS OF CRESCENT WINGS USING A SUBSONIC PANEL METHOD

C.W.Burkett*
Department of Aeronautics and Astronautics,
University of Southampton, England

Abstract

Recent experimental and computational studies have indicated that rearward curvature of a wing can reduce the induced drag factor to values less than that obtained from the unswept elliptical wing considered optimal in classical wing theory. The origin of this induced drag reduction is investigated by using a three-dimensional panel method which features a wake relaxation routine to model the non-linear behaviour of the trailing wake. The effect of wake non-planarities is assessed by comparing rigid and relaxed wake solutions. Results showed reductions in induced drag factor of up to 16% for wings with rearward curvature. Wake relaxation consistently gave increased drag compared to the planar wake case, but the detrimental effect was reduced for wings of rearward curvature. Sectional drag data demonstrates that rearward planform curvature encourages a thrust force at the tips whilst minimising the high drag at the root found on wings of constant sweep.

Nomenclature

AR	aspect ratio, b^2/S
b	wing span
c	local wing chord
C_d	sectional drag coefficient
C_D	drag coefficient
C_{Di}	induced drag coefficient
C_l	sectional lift coefficient
C_L	wing lift coefficient
C_p	pressure coefficient
C_x, C_z	local force coefficients
e	span (or induced) efficiency factor
K	induced drag factor(1/e)
p,q,r	Cartesian coordinate variables, orientated relative to the free-stream velocity vector
S	wing area
U_∞	freestream velocity
x,y,z	Cartesian co-ordinate system variables, body fixed
x_t	x-co-ordinate of the tip location (expressed in root chord lengths behind the root leading edge)
α	angle of attack
η	y/(b/2), non-dimensional spanwise co-ordinate

Introduction

There are many examples in nature of animals who require a highly efficient means of locomotion adopting a crescent-shaped planform for their wings or tail surfaces. Dolphins and the fastest swimming fish have lunate, or crescent-shaped tail fins. The albatross and other seabirds who soar over long distances typically have high aspect ratio wings with tapered, aft swept tips. The swift, which spends most of its life airborne, also employs a crescent-shaped planform. The widespread adoption of the crescent shape after many millions of years of evolution is surprising since, according to classical theory, the minimum induced drag of a planar, untwisted lifting surface is obtained from an unswept wing of elliptical planform.

Determination of the induced drag for a configuration is traditionally conducted in the Trefftz plane from a knowledge of the spanwise loading alone. A Trefftz plane analysis relies upon the wake retaining its original shape so that induced drag may be calculated infinitely far downstream. The wake shed by a planar wing is therefore modelled as a flat trailing vortex sheet, extending infinitely far downstream and lying parallel to the x-axis (Fig.1). Trefftz plane analysis leads to the familiar result, first derived by Munk[1], that an elliptic spanwise loading is necessary for minimum induced drag which, for the unswept planar wing of constant section, may in turn be generated by an elliptical distribution of chord across the span. Prandtl[2] showed that the minimum drag condition is given by the well known relationship $C_{Di} = Cl^2 / \pi . AR$. Any departure from the elliptical loading inevitably leads to higher induced drag factors.

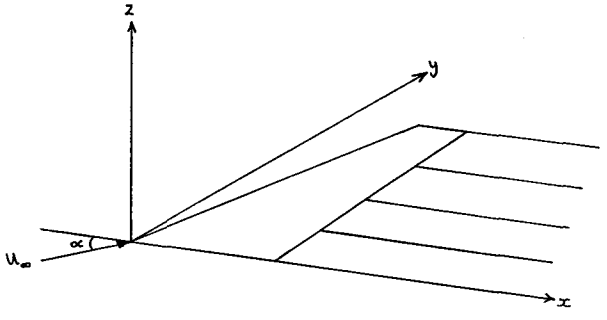

Fig.1 Classical representation of a lifting surface and its wake

* currently Aerodynamicist with Leyton House Racing Ltd.

The Trefftz plane technique has been applied with considerable success to unswept wings, but tends to be less reliable for swept wings. There are several approximations inherent in the linearised theory which begin to become significant in the latter case.

The standard wake model employed implies that the effects of wake non-planarities and vortex roll-up along its free edges are small enough to be ignored. However, as the wing departs further from the unswept planform, the assumption of a planar trailing wake becomes progressively less valid. The requirement for the wake to be force-free causes it to "relax" from a rigid sheet in the x-plane and adopt a freestream orientation. This is an important physical characteristic of the flow which is not modelled by classical theories; it is this characteristic which allows a planar, swept wing to generate a non-planar wake. Furthermore, only specially designed wings will produce trailing vortex sheets which move downward at a constant speed. If downwash varies across the span, the vortex sheet must deflect under its own influence. These two factors are in addition to the well known roll-up of the vortex sheet into a pair of counter-rotating tip vortices within a few chord lengths of the wing, which inevitably increases the induced drag.

No knowledge of wing planform shape is required for the induced drag calculation in the Trefftz plane. The implication, therefore, is that downwash from the trailing vortices is independent of the angle of sweep and remains the same whether the streamwise vortices are staggered or not. This is clearly not the case, and this drastic simplification must imply some errors. Furthermore, no account is taken of the significant redistribution of sectional drag over the surface of swept wings, due primarily to the behaviour of the bound vortices. The benefits to be gained from exploiting this behaviour cannot be predicted from the traditional Trefftz plane approach.

The limitations of the Trefftz plane approach can be overcome through the use of panel methods featuring a wake relaxation routine. A rapidly converging iterative procedure models the non-planar property of the trailing wake by aligning the vortex lines with the local flow direction, thereby ensuring that the wake carries no load. Lift and drag are calculated directly by integration of the surface pressures. Any changes in the induced drag arising from modifications made to the planform or wake shape can clearly be associated with modifications to the sectional pressure distributions. The disadvantage of this approach is that the accuracy of lift and drag data depends upon numerical integration of the pressure distribution from a number of discrete data points. Careful attention to panelling detail is necessary to ensure that the full pressure distribution is satisfactorily captured.

This paper investigates the origin of the induced drag benefits claimed for the crescent wing. A summary of previous experimental and computational studies is provided, which shows that wake non-planarities have always been cited as the source of the benefits. By using a three dimensional panel method with a wake relaxation option, a direct comparison is made between solutions with rigid and with relaxed wakes. Examination is also made of the influence of the crescent planform itself on both chordwise and spanwise loading. Comparison with a wing of constant sweep clearly demonstrates in terms of surface pressures how a crescent wing is able to reduce induced drag.

Previous Experimental and Computational Studies

Zimmer, in a study of wings with aft-swept tips[3], realised that these planforms shed significantly non-planar trailing wakes. This effect is caused by the downward displacement of the wing tip relative to the root when the wing is inclined at an angle of attack (Fig.2). Zimmer used a vortex-lattice method to study the induced drag of a variety of wing planforms. The theoretical model featured a non-linear wake with the trailing vortices kinked into the freestream direction a half-chord length behind the trailing edge. Using this method a figure of K=0.976 was obtained for a rectangular wing with an aft-swept triangular tip. A similar planform has since been successfully employed by Dornier on their 228 commuter aircraft.

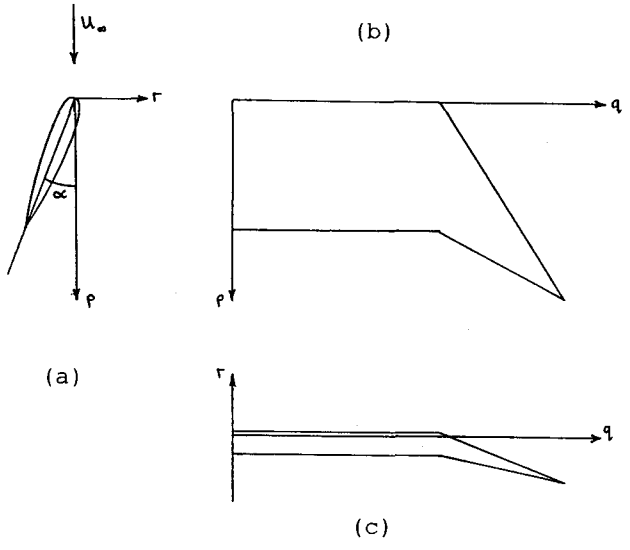

Fig.2 Sketch of a wing with an aft swept tip at angle of attack: (a) root chord, (b) plan view, (c) rear view showing the vertical displacement of the tip relative to the root

By way of explanation for the low drag figures obtained from wings with aft swept tips, Zimmer considered the shape of the foremost bound vortex, and its projection onto a "Trefftz" plane normal to the freestream. Non-planarity, due to the aft-swept tip, resulted in the theoretically attainable induced drag, assuming an optimum load distribution, falling below the value for a planar bound vortex trace of the same span. Zimmer's justification for considering the shape of the foremost bound vortex was that the results from his vortex lattice theory indicated a close correlation between the sectional induced drag and the circulation distribution along this bound vortex.

The author[4] recently extended these ideas and introduced the concept of planform-camber equivalence to assess the influence of wake non-planarities induced by a variety of wing planforms. A bound vortex placed along the quarter chord line of a wing at angle of attack can, by Munk's stagger theorem, have each vortex element along its length translated in a freestream direction to yield an equivalent non-planar vortex arc lying in a plane normal to the freestream. In this way the effect of planform on a lifting line model can be regarded as an in-plane curvature. Using solutions provided by Cone[5] for the minimum induced drag of various non-planar lifting systems, the crescent wing was identified as the planform to derive the most benefit from its non-planar wake shape, typically a 4% reduction in induced drag factor at moderate incidence.

Further studies have been conducted by van Dam[6,7], who has analysed wings with aft swept tips and a family of crescent planforms using the panel method VSAERO. Using a wake relaxation routine to model the non-planar wake, a value of K = 0.919 was predicted for a crescent wing with its tip located 1.5 root chord lengths behind the root leading edge. Wind tunnel tests of a similar planform in the NASA Langley 14- by 22-foot tunnel[8] showed a reduction in induced drag factor of around 3% compared to an unswept elliptical wing. Also of interest was the high angle of attack behaviour of the crescent wing[9]; maximum lift was 8% higher and post-stall behaviour improved. Flow visualisation studies indicated that the lift increment was the result of leading edge separation-induced vortex flow over the highly swept tip regions of the crescent wing. These results are supported by tests conducted last year in the 7'x5' wind tunnel at the University of Southampton[10]. Tuft studies of the Dornier 228 wing have also shown that its aft swept tips remain unstalled well after the inboard wing has stalled[11].

A Study of Crescent Wing Planforms Using the Panel Method SPARV

To provide a clearer understanding of the flow behaviour over the surface of a crescent wing, a family of wings similar to that studied by van Dam was analysed using the panel method SPARV at British Aerospace Commercial Aircraft Division, Hatfield. These planforms, of aspect ratio 6, are characterised by semi-elliptical leading and trailing edges, along with an elliptical distribution of chord (Fig.3). The planform with a straight quarter chord line (x_t = 0.25) represents an unswept elliptical wing considered optimal in classical theory.

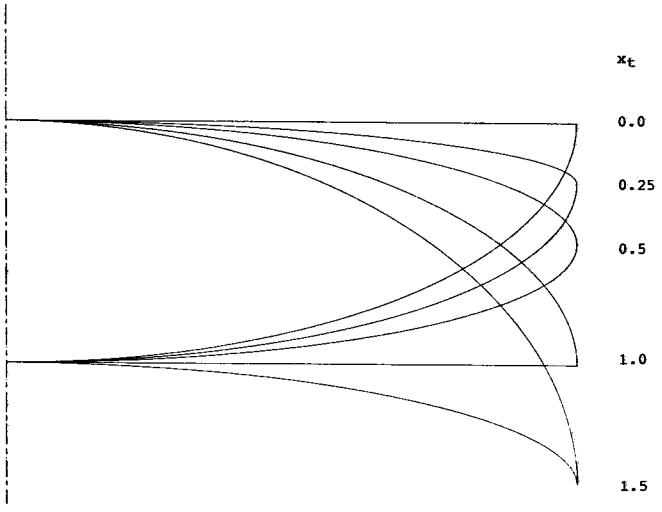

Fig.3 The family of planforms analysed using the panel method SPARV

SPARV[12] is a three dimensional surface source and doublicity panel method which, like VSAERO, models the non-linear behaviour of the wake by using a wake relaxation procedure. The lift and the induced drag of a configuration are determined directly from integration of the pressure distribution. The problem of separating the overall drag into its constituent components does not arise since, in inviscid flow, the only drag component generated is induced drag. By using a NACA 0012 aerofoil with a symmetrical section, the induced drag factor K may easily be evaluated using the relationship:

$$K = \pi.AR.C_{Di}/C_L^2$$

The performance of the panel method, and its sensitivity to variations of panelling geometry, was assessed by using the unswept elliptical wing as a test case. According to classical theory, an induced drag factor of unity should be obtained, along with an elliptical spanwise load distribution. In addition, use of a symmetrical section should result in zero lift and zero drag at zero incidence. Since SPARV calculates the lift and drag by integration of the pressure

distribution, it is of critical importance that the panelling of the wing is sufficiently dense to fully capture both the spanwise and chordwise variations, particularly around the leading edge. Poor results for the elliptical test case planform would be indicative of poor panelling.

Analysis revealed that approximately 100 chordwise panels were necessary to satisfactorily capture the pressure distribution; these were distributed in a full cosine distribution to give sufficient panel density near leading and trailing edges. The number of spanwise panels was less critical; 16 panels were used to ensure adequate definition of the planform geometry and spanwise loading variations. A pure elliptical wing has zero tip chord, and faithful reproduction of such a planform leads to panel aspect ratio problems near the tip. It was found that for realistic spanwise panel densities the minimum acceptable tip chord was about 10% of the root chord. Although this may appear to be a significant departure from the elliptical chord distribution, truncation at the tip is barely detectable- the modification is equivalent to the loss of the outermost 0.5% of the semispan. All force coefficients were calculated on the basis of the cropped planform area.

The necessity of using finite tip chords introduces a further panelling problem, namely that of flow leakage at the tip. The upper and lower surface singularity sheets no longer meet at the tip, allowing flow to "leak" into and out of the hollow wing. SPARV analysis showed that closing the tip to avoid the problem was necessary. The outermost upper and lower surface panels were therefore angled towards each other to join along the centreline of the aerofoil section.

The unswept elliptical wing was analysed, initially with a rigid wake, at incidences of zero and four degrees, giving the following results:

α = 4 deg C_L = 0.3333 C_D = 5.995×10^{-3}
α = 0 deg C_L = 1.5×10^{-10} C_D = 0.1×10^{-3}

The calculated lift coefficient is 1.8% greater than the lift coefficient calculated using van Dyke's expression for the lift curve slope for elliptical wings of moderate-to-high aspect ratio[13]. The spanwise load distribution was so close to a pure elliptical loading that the plot shown in Fig.4 fails to distinguish between the two. At zero incidence, the drag coefficient is less than 2% of its value at 4 degrees, and the lift coefficient is negligible. Correcting the values at 4 degrees for the zero error gives an induced drag factor of K = 0.995. The considerable attention paid to careful panelling was thus rewarded by excellent results for the unswept elliptical wing.

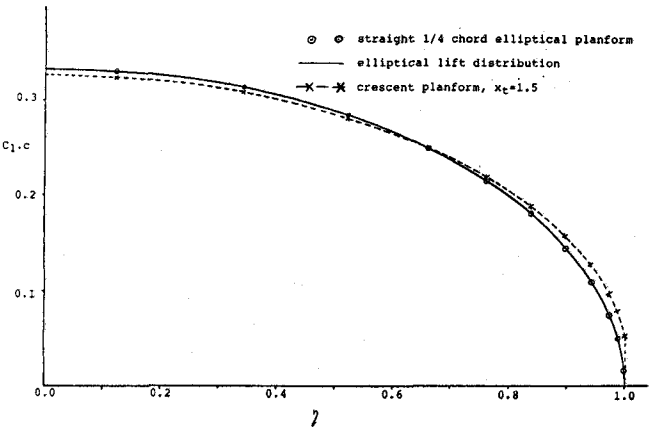

Fig.4 SPARV spanwise loading for an unswept elliptical wing and a crescent planform

Results for a Family of Crescent Wings

The panelling geometry described above was used with each planform to ensure that changes in performance could not be attributable to changes in panelling. Analysis was conducted at 4 degree incidence with both rigid and relaxed wake geometries, along with a zero incidence correction run for each planform. The variation of induced drag factor is presented in Fig.5; each result includes the corresponding zero incidence correction.

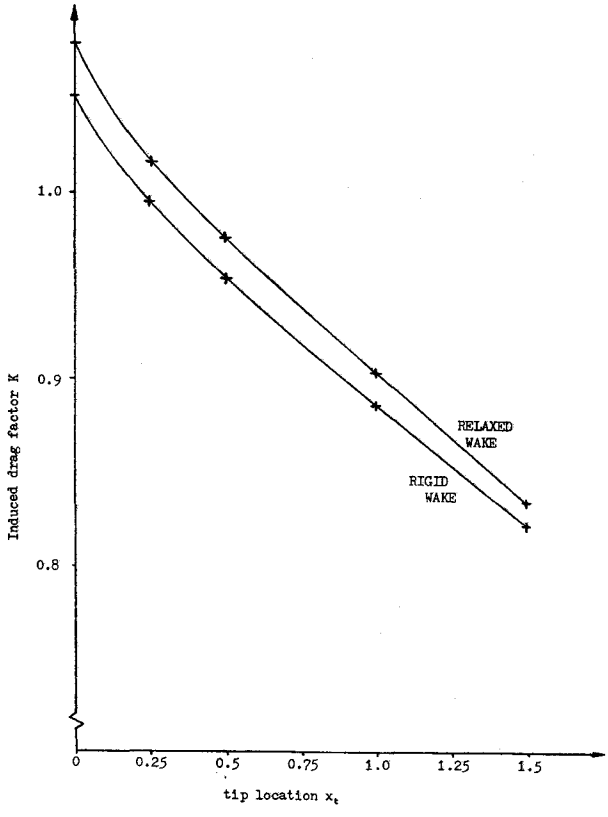

Fig.5 Variation of induced drag factor with tip location

Results show significant reductions in induced drag factor as the tip location moves rearwards, down to values as low as 0.834 (relaxed wake) at x_t = 1.5. This compares with the value K = 0.919 obtained by van Dam. Of particular interest is the fact that wake relaxation was not necessary in order to predict drag reductions for the crescent wing planforms; in fact, the relaxed wake solutions consistently gave higher induced drag factors. A 2.2% increase in K resulted from relaxation of the wake associated with the unswept wing. This increase progressively reduced as rearward sweep increased, with a difference between rigid and relaxed wake solutions of 1.2% when x_t = 1.5. These results were particularly surprising since previous studies had consistently associated the reductions in induced drag factor with the non-planar property of the trailing wake. Closer examination of van Dam's figures showed, however, that VSAERO also predicted a similar behaviour, with increases in K of 4.6% and 0.7% respectively when wake relaxation was applied to the two planforms described above. For the unswept wing, changes in the induced drag factor as a result of wake relaxation give an indication of the effect of vortex roll-up along the edge of the sheet. The formation of a tip vortex, with high induced rotational velocities, interferes with the ideal constant downwash distribution leaving the trailing edge of the unswept elliptical wing, resulting in an increase of induced drag factor of a few percent. A tip vortex will also be formed downstream of the crescent wing, leading to a similar increase in induced drag factor. For the crescent

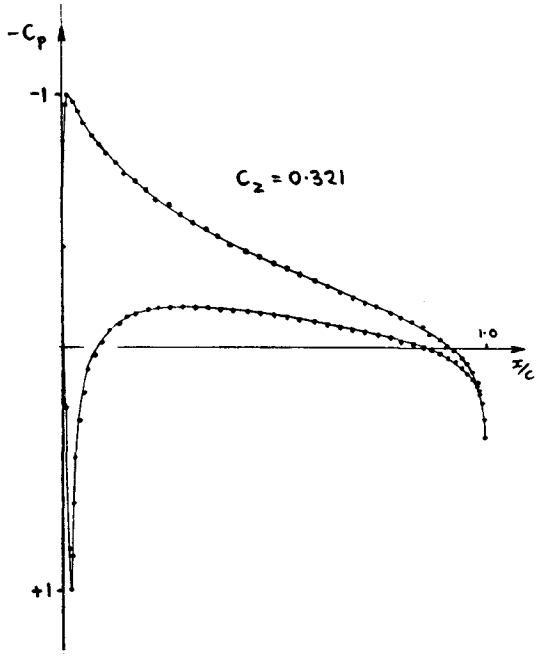

Fig.6(a)

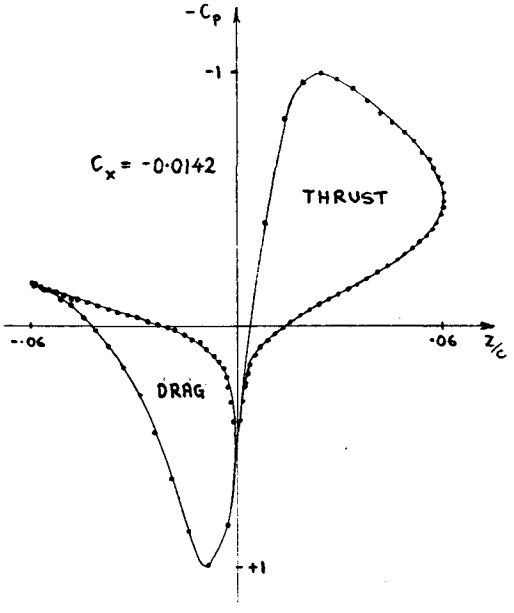

Fig.6(a) cont.

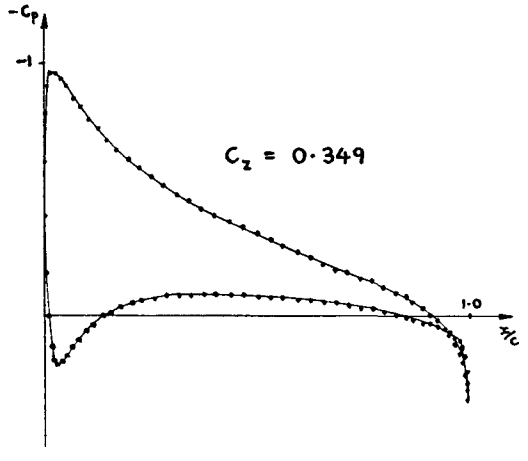

Fig.6(b)

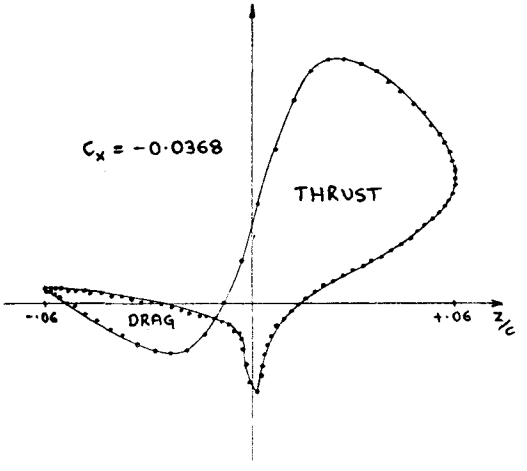

Fig.6(b) cont.

Fig.6 SPARV spanwise pressure plots for the crescent wing (x_t=1.5) at: (a) 10% semispan, (b) 92.9% semispan

wing, however, there is an additional non-planarity introduced into the wake by virtue of the aft swept tip (as shown in Fig.2). The results from both SPARV and VSAERO demonstrate that this non-planarity serves to reduce the overall detrimental influence of wake relaxation by between 1% and 4%. The magnitude of the effect compares favourably with that predicted by the author using the planform-camber equivalence principle of Ref.4.

Spanwise loading associated with the crescent wing (x_t =1.5) is compared with the elliptical loading in Fig.4. A super-elliptic loading, with higher loading near the tip, is to be expected from wings with rearward sweep.

Pressure distributions predicted by SPARV are sensible, with well defined suction peaks. The high chordwise panelling density ensured that errors in lift coefficient introduced through inaccurate numerical integration of the pressure distribution are minimal. The drag loops predicted by SPARV are similarly well defined, minimising errors in drag coefficient. Sample pressure distributions and drag loops are shown in Fig.6 for the crescent wing (x_t = 1.5) at spanwise stations η = 0.1 and η = 0.929. The SPARV pressure distributions are typical of those obtained from an inviscid theory.

The most striking difference between the results at the two spanwise stations is the erosion of the lower surface stagnation pressure at the outer station. Since this is the main cause of the pressure drag on an aerofoil section, the sectional drag decays, and becomes a thrust near the tips. This is evidenced by the decay of the drag loop and the expansion of the thrust loop, as shown in Fig.6.

Comparison with Wings of Constant Sweep

It is informative to compare the behaviour of the crescent wing with that seen on a wing of constant sweep. A crescent wing may be considered to be composed of an unswept central section and a highly swept outboard section, with a smooth transition between the two. Significant redistributions of drag over the surface of swept wings arise from strong root and tip effects. Departure from the two dimensional pressure distribution at the root and tips is evidenced by the isobar pattern existing over the surface of a swept wing, typically as shown in Fig.7. In both regions the isobars are straightened out, which affects the chordwise loadings and the sectional lift slopes. Whereas the centre effect shifts the minimum pressure backward along the chord of a sweptback wing and usually reduces it slightly, the tip effect shifts it forward and usually makes the suction peak higher. This departure of the pressure distribution from that of an infinite sheared wing implies that a normal pressure drag acts at the centre of a sweptback wing and a thrust at the tips, because zero drag is obtained only with pressure distributions as on two dimensional aerofoils. The pressure distribution over a sweptback wing would typically appear as in Fig.8.

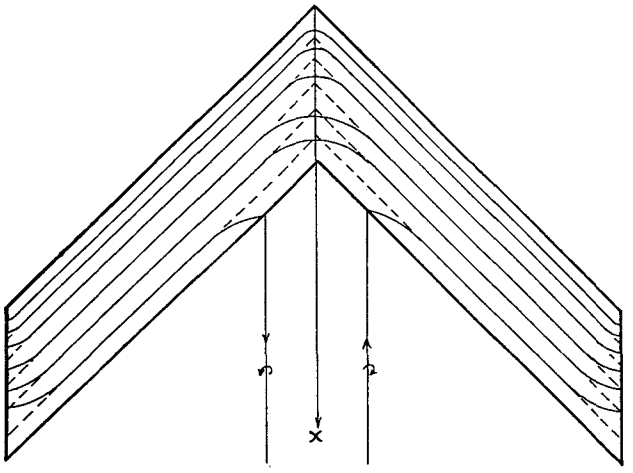

Fig.7 Typical isobar pattern over the surface of a swept wing of large aspect ratio (adapted from Ref.14)

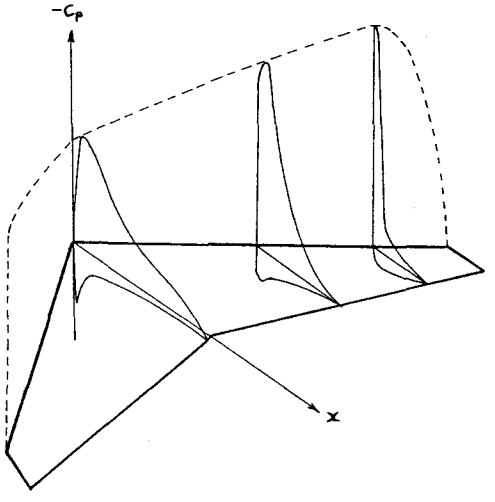

Fig.8 Typical pressure distributions over a sweptback wing (adapted from Ref.14)

The distorted chordwise load distributions at the centre and the tips give rise to an additional local drag or thrust, ΔC_D, proportional to C_L^2. The actual values of ΔC_D can be considerable; ΔC_D at the root may be ten times the ordinary profile drag. Whilst ΔC_D integrated over the span is zero, the very high local drags and thrusts are in a precarious balance over the surface of the swept wing. The thrust force depends on the high suction peaks near the tips, and the loss of a fraction of this thrust

means a big increase in drag. This explains why the drag rise is large as soon as there is any breakdown in the forward peak suctions at the tip, which may occur while the overall lift is still rising.

The primary motivation for using wing sweep has been to increase the drag rise Mach number of high speed aircraft. Since critical conditions are reached only when the local velocity component normal to the isobars reaches the local speed of sound, design of swept wings has been dominated by the necessity to maintain a constant isobar sweep across the span from root to tip. The tendency of the isobars to straighten in both the root and the tip regions has had to be countered by the use of the well known "Kuchemann tips" and by flaring the root leading edge into the fuselage. With low speed aircraft, however, constant isobar sweep is unnecessary and may even be undesirable.

It is noted in Refs.14 and 15 that the Kuchemann tip appears to yield benefits at subsonic, as well as supersonic speed. Such a tip shape capitalises on the thrust forces generated at the tip of a swept wing. On a swept wing with a square-cut tip, these thrust forces are generated by "peaky" pressure distributions with large suctions near the leading edge; in a viscous flow the adverse pressure gradient behind such a suction peak is very liable to provoke a boundary layer separation, which in turn reduces the section circulation. This causes a collapse of the suction peak and a substantial reduction in the local thrust force, leading to a corresponding increase in the overall drag. On a wing with a curved tip, a local thrust force is produced by reducing the positive pressures, and not by increasing the upper surface suction. The prospect of realising such a thrust force in the real viscous flow is thereby improved. This behaviour is clearly illustrated over the curved tip of a crescent wing by the pressure distributions obtained from SPARV, and shown in Fig.6. The substantial reduction in the positive pressures near the attachment line is evident, along with the accompanying erosion of the sectional drag loop.

It would seem reasonable to aim to minimise the large drag forces at the centre section in much the same way that the thrust forces at the tip were encouraged through the use of the Kuchemann tip. Methods are therefore required to modify the plain swept wing so as to encourage a more two-dimensional character at the root. It is proposed that this may be achieved by progressively reducing wing sweep as the root is approached, until the wing is locally unswept on the centre-line. In this manner, the wing planform itself is effectively being modified to follow the local isobar sweep at the root. The result is a wing with rearwards curvature; if an optimum distibution of chord is superimposed along the span, a crescent wing results. The benefits which appear to be gained by reducing the sweep at the root simply mirror the benefits gained by increasing the sweep at the tip.

Fig.9 shows the local drag forces for elliptical and crescent wings obtained from SPARV compared with Kuchemann's data[12] for a 45 degree swept wing; his data has been scaled by the factor $(C_L^2/AR)_{sparv}/(C_L^2/AR)_{Kuchemann}$ since the lift coefficent and the aspect ratio of Kuchemann's test is different from the values to which the SPARV results correspond. Results appear consistent with the philosophy described above; the crescent wing successfully eliminates the high sectional drag at the root. Over the central portion of the wing, Fig.9 indicates that the 45 degree swept wing is superior, with the crescent wing providing higher thrust forces over the outer 20% of the semispan. This behaviour seems reasonable, since the outer sweep of the crescent wing is very high, which will result in a stronger tip effect. The generally consistent results shown in Fig.9 seem to support the validity of the results obtained from SPARV.

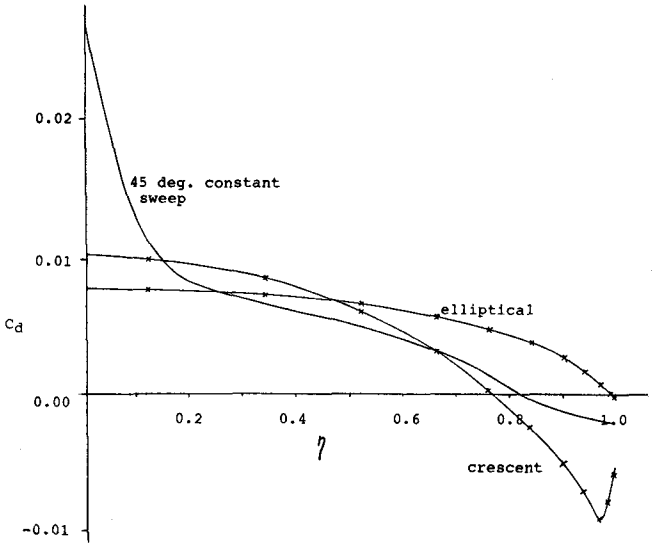

Fig.9 Sectional drag in inviscid flow for an elliptical wing and a crescent wing (from SPARV) and for a 45 deg. swept wing (from data in Ref.14)

Conclusions

Analysis of a family of crescent wings using a three dimensional panel method predicts significant reductions in induced drag compared to an unswept elliptical planform, both with and without relaxation of the planar wake. Induced drag factor fell to a value of K=0.834 with the tip located 1.5 root chord lengths behind the root leading edge. Wake relaxation

consistently led to increased induced drag compared to the planar wake case, due to the undesirable influence of vortex roll-up near the tips. However, as tip location moved rearwards the increase in induced drag due to wake relaxation was reduced. It is suggested that this is due to the beneficial influence of wake non-planarities induced by wings with aft swept tips when operated at an angle of attack (Fig.2).

The flow behaviour over a crescent wing was compared with that over a wing of constant sweep, which typically has large drag forces at the root and a thrust force at the tip. Examination of the sectional drag distribution showed that the crescent wing achieves its reduction in induced drag by minimising the drag at the root, and encouraging the thrust force at the tip. Reduction in sweep at the root encourages a two-dimensional character; the planform is effectively modified to follow local isobar sweep at the root. Increasing sweep at the tip promotes the local thrust force by reduction of positive pressures around the lower leading edge, in much the same way as the well known "Kuchemann tip".

Acknowledgements

The author would like to acknowledge the provision of computing facilities by British Aerospace Commercial Aircraft, Hatfield, and the assistance provided members of the Research Department.

References

1. Munk,M.M. "The Minimum Induced Drag of Aerofoils." NACA Report 121, 1921.

2. Prandtl,L. "Applications of Modern Hydrodynamics to Aeronautics." NACA Report 116, 1921.

3. Zimmer,H. "The Aerodynamic Optimisation of Wings at Subsonic Speeds and the Influence of Wingtip Design." NASA TM-88534, 1987.

4. Burkett,C.W. "Reductions in Induced Drag by the Use of Aft Swept Tips." Aeronautical Journal, December 1989, pp. 400-405.

5. Cone,C.D.,Jr. "The Theory of Induced Lift and Minimum Induced Drag of Nonplanar Lifting Systems." NASA TR R-139, 1962.

6. van Dam,C.P. "Swept Wing-Tip Shapes for Low-Speed Airplanes." SAE Paper 851770, 1986.

7. van Dam,C.P. "Induced-Drag Characteristics of Crescent-Moon-Shaped Wings." Journal of Aircraft, vol.24, no.2, Feb.1987, pp.115-119.

8. van Dam,C.P., Vijgen,P.M.H.W. and Holmes,B.J. "Wind Tunnel Investigation on the Effect of the Crescent Planform Shape on Drag." AIAA Paper 90-0300, 28th Aerospace Sciences Meeting, Reno, Nevada, January 8-11, 1990.

9. van Dam,C.P., Vijgen,P.M.H.W. and Holmes,B.J. "High-α Characteristics of Crescent and Elliptic Wings." AIAA Paper 89-2240, AIAA 7th Applied Aerodynamic Conference, Seattle, WA, July 31-August 2, 1989.

10. Burkett, C.W. "Reductions in Induced Drag by the Use of Aft Swept Wing Tips." BEng. project report, Dept.of Aeronautics and Astronautics, University of Southampton, May 1989.

11. Welte,D., Birrenbach,R. and Haberland,W. "Wing Design for Lift Transport Aircraft with Improved Fuel Economy." Zeitschift Fur Flugwissenschaften und Weltraumforschung, no.5, 1981, pp.294-303.

12. Petrie,J.A.H. "Development of an Efficient and Versatile Panel Program for Aerodynamic Problems." Leeds University Doctoral Thesis. March 1979.

13. Van Dyke,M. Perturbation Methods in Fluid Mechanics, Parabolic Press, Stanford, CA, 1975, Note 13.

14. Kuchemann,D. The Aerodynamic Design of Aircraft. Pergamon Press, 1978.

15. Weber,J. "Low Speed Measurements of the Pressure Distribution near the Tips of Swept Wings at No Lift." RAE Report Aero. 2318. A.R.C. 12,241, 1949.